Compensation of chromatic dispersion for full-duplex ROF link with vector signal transmission using an optical phase shifter

Chao Gao (高 超)*, Shanguo Huang (黄善国), Jinghua Xiao (肖井华), Xinlu Gao (高欣璐), Qian Wang (汪 茜), Yongfeng Wei (魏永峰), Wensheng Zhai (翟文胜), Wenjing Xu (徐文静), and Wanyi Gu (顾畹仪)**

State Key Laboratory of Information Photonics and Optical Communications, Beijing University of Posts and Telecommunications, Beijing 100876, China

**Corresponding author: gaochao19830606@bupt.edu.cn;*

***corresponding author: shghuang@bupt.edu.cn*

Received July 11, 2014; accepted October 24, 2014; posted online January 5, 2015

We demonstrate the theory of chromatic dispersion (CD)-induced constellation rotation (CR) in a radio-over-fiber (ROF) link and a method for compensation. We also propose a 60 GHz full-duplex ROF system with vector signal transmission including no CD effect. The evaluation of 5 Gb/s 16 quadrature amplitude modulation signal transmission shows that the CD-induced CR can be entirely overcome due to the proposed method which is simply implemented through an optical phase shifter. The proposed ROF schedule is not only applicable for V-band (57–64 GHz) but also fits for W-band (75–110 GHz), or any other bandwidth.

OCIS codes: 060.4510, 060.5625.

doi:10.3788/COL201513.010604.

With the rapid growth in demand for distribution of high-capacity wireless signals, radio-over-fiber (ROF) technique that builds broadband wireless and wired connectivity has become a promising application area for analog optical links[1–7]. Compared with the conventional 802.11n (2.4 or 5 GHz), V-band (57–64 GHz) and W-band (75–110 GHz) have attracted much interest due to larger available bandwidth.

Chromatic dispersion (CD) has always been a significant impairment in long ROF link[8–11]. It causes each spectral component to experience different phase shifts, and produce a phase difference between the two beat signals, which results in an unwanted phase at the radio frequency (RF). When it comes to ROF links with high spectral efficiency vector signal transmission, CD-induced unwanted phase will cause a constellation rotation (CR) effect to the RF vector signal, which greatly lowers the quality of the transmission signals and brings trouble to subsequent transmission, demodulation, and digital signal processing (DSP).

Many researchers have focused on CD compensation for ROF links[12–15]. However, some of the schemes need expensive equipment and complex architecture, which will extremely increase costs of the whole system. Because of the large loss in the air, numbers of base stations (BSs) are indispensable to realize the seamless coverage of a ROF network. It is always a big deal that much attention should be paid to the costs of a ROF system. Meanwhile, DSP techniques are also used for CD compensation in ROF links. However, DSP always reaches a certain function in the cost of distorting the original data, which is evitable, or unacceptable in some circumstance.

In this letter, we demonstrate the theory of CD-induced CR in ROF link and a method for compensation. A 60 GHz full-duplex ROF system with vector signal transmission including no CD effect is proposed as well. The evaluation of the system with 5 Gb/s 16 quadrature amplitude modulation (QAM) signal transmission shows that the CD-induced CR is entirely overcome thanks to our method which can be simply implemented through an optical phase shifter (OPS), without any expensive equipment, complex architecture, or DSP techniques to distort transmission signals for CD compensation.

In a ROF system, most of signal processing functions can be completed in the central station (CS) with much of the equipment centralized and co-shared, so that the remote BS is significantly simplified and cost-effective. A full-duplex ROF link with vector signal transmission and CD compensation is proposed (Fig. 1).

Laser diode (LD) emits the lightwave $E_0(t) = E_0\cos(\omega_0 t)$, and double-sideband (DSB) carrier suppression modulated by a local oscillator (LO) as $V_{\mathrm{LO}}(\mathrm{t}) = V_{\mathrm{LO}}\cos(\omega_{\mathrm{LO}} t)$ via a dual drive Mach–Zehnder modulator (MZM) to generate two sidebands, the upper sideband (USB) and the lower sideband (LSB), which can be expressed as

$$E_1(t) = \frac{E_0}{2}\cos\left[\omega_0 t + m_{\mathrm{LO}}\cos\left(\omega_{\mathrm{LO}} t\right) + \pi\right] + \frac{E_0}{2}\cos\left[\omega_0 t + m_{\mathrm{LO}}\cos\left(\omega_{\mathrm{LO}} t + \pi\right)\right]$$

$$\approx E_0 J_1(m_{\mathrm{LO}})\left[\sin\left(\omega_0 t - \omega_{\mathrm{LO}} t\right) + \sin\left(\omega_0 t + \omega_{\mathrm{LO}} t\right)\right], \quad (1)$$

where $m_{\mathrm{LO}} = V_{\mathrm{LO}}/V_\pi$ is the modulation index and $J_n(m_{\mathrm{LO}})$ is the nth-order Bessel function of the first kind. We neglect

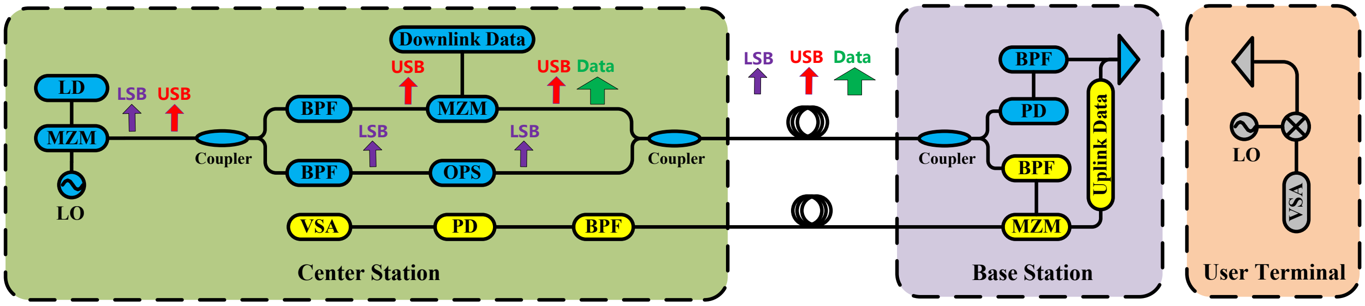

Fig. 1. Full-duplex ROF link with vector signal transmission and CD compensation.

the higher order sidebands since the modulation index is small.

The USB and LSB are separated by two band pass filters (BPFs) and the USB is single-sideband (SSB) modulated by downlink 16 QAM vector signal, which can be represented as $S(t)=A(t)\cos\left[\omega_S t+\theta_S(t)\right]$, where $A(t)$ and $\theta_S(t)$ are the symbol's amplitude and phase in constellation and ω_S is angular frequency of downlink signal. The output of the second MZM can be expressed as

$$\begin{aligned}E_2(t)=&\frac{E_0}{2}J_1(m_{LO})\sin\left\{\omega_0 t+\omega_{LO}t+m_A\cos\left[\omega_S t+\theta_S(t)\right]+\frac{\pi}{2}\right\}\\&+\frac{E_0}{2}J_1(m_{LO})\sin\left\{\omega_0 t+\omega_{LO}t+m_A\cos\left[\omega_S t+\theta_S(t)+\frac{\pi}{2}\right]\right\}\\&\approx\sqrt{2}/2E_0J_1(m_{LO})\sin\left(\omega_0 t+\omega_{LO}t+\pi/4\right)\\&-E_0J_1(m_{LO})\ A(t)\sin\left[\omega_0 t+\omega_{LO}t+\omega_S t+\theta_S(t)\right],\qquad(2)\end{aligned}$$

where $m_A=\pi A(t)/V_\pi$ is the second modulation index. We take the approximation $J_1(m_A)\approx m_A\approx\ A(t)$ since the second modulation index is also small.

The LSB is transmitted without data modulation, and we ignore the OPS for now. The three tones are combined by an optical coupler after aligning the polarization direction by polarization controller, and transmitted over the single-mode fiber (SMF), which can be represented as

$$\begin{aligned}E_3(t)&=E_{LSB}(t)+E_{USB}(t)+E_S(t)\\&=E_0J_1(m_{LO})\sin\left(\omega_0 t-\omega_{LO}t\right)\\&+\sqrt{2}/2E_0J_1(m_{LO})\sin\left(\omega_0 t+\omega_{LO}t+\pi/4\right)\\&-E_0J_1(m_{LO})\ A(t)\sin\left[\omega_0 t+\omega_{LO}t+\omega_S t+\theta_S(t)\right].\qquad(3)\end{aligned}$$

At the photodiode (PD), the beating between $E_S(t)$ and $E_{LSB}(t)$ can produce the required radio millimeter wave.

In fact, if CD is taken into account, each spectral component will experience different phase shifts depending on the fiber–link distance, modulation frequency, and the fiber dispersion parameter. These phase shifts result in a phase difference between the data sideband and the LSB, and produce an unwanted phase at the RF, which will greatly lower the quality of the vector signals. Apart from wavelength division multiplexing system or specialized analysis, higher order dispersion is always discarded in normal ROF links because of its non-primary status for vector signal transmission. The CD impact factor for a fiber link can be expressed as[16]

$$\theta=\frac{1}{2}\beta_2\Omega^2L,\qquad(4)$$

where Ω is angular frequency of modulation signal, L is the length of the fiber, and β_i is the ith order transmission constant of the fiber. Here we have neglected polarization dispersion and fiber nonlinearities.

Illustration of CD compensation for downlink is shown in Fig. 2. No extra phase difference occurs in the link while CD is ignored (Figs. 2(a1), (b1), and (c1)). If taking CD into account, the data sideband and the LSB have the same initial phases before transmission (Fig. 2(a2)). The dispersive transmission introduces a phase shift θ_1 to both USB and LSB, and a phase shift θ_2 to data sideband (Fig. 2(b2)), which satisfies

$$\theta_1=\frac{1}{2}\beta_2\omega_{LO}{}^2L,\qquad(5)$$

$$\theta_2=\frac{1}{2}\beta_2\left(\omega_{LO}+\omega_S\right)^2L.\qquad(6)$$

Considering the CD impact factor, Eq. (3) can be rewritten as

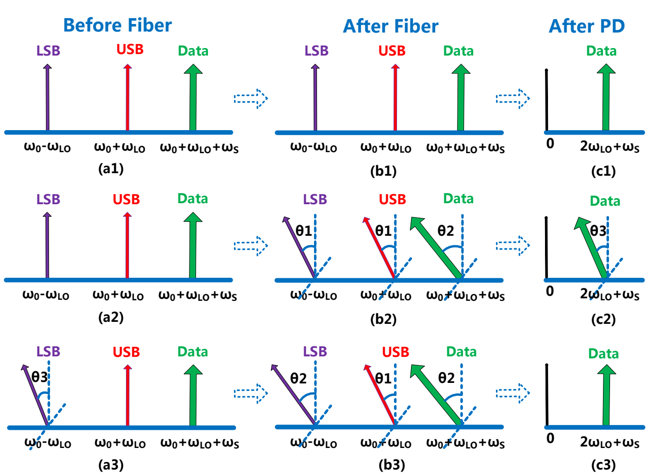

Fig. 2. Illustration of CD compensation for downlink.

$$E_4(t) = E_0 J_1(m_{LO})\sin(\omega_0 t - \omega_{LO} t + \theta_1)$$
$$+\sqrt{2}/2E_0 J_1(m_{LO})\sin(\omega_0 t + \omega_{LO} t + \pi/4 + \theta_1)$$
$$-E_0 J_1(m_{LO})\ A(t)\sin[\omega_0 t + \omega_{LO} t + \omega_S t + \theta_S(t) + \theta_2]. \quad (7)$$

The electric signal after PD can be expressed as

$$I(t) = \text{BPF}\left[|E_4(t)|^2\right]$$
$$= E_0^2 J_1^2(m_{LO}) A(t)\cos[(2\omega_{LO} + \omega_S)t + \theta_S(t) + (\theta_2 - \theta_1)], \quad (8)$$

where BPF[*] represents filtered by BPF. It can be seen from Eq. (8) that CD leads to an extra phase θ_3, as shown in (Fig. 2(c2)), which satisfies

$$\theta_3 = \theta_2 - \theta_1 = \frac{1}{2}\beta_2\left[(\omega_{LO} + \omega_S)^2 - \omega_{LO}{}^2\right]L. \quad (9)$$

If an initial phase θ_3 is given to the LSB by OPS before transmission (Fig. 2(a3)), the relative phase between the LSB and the data sideband is zero after transmission (Fig. 2(b3)). There is no unwanted phase after PD (Fig. 2(c3)).

For the uplink, the USB and LSB are filtered out at the BS by a BPF as the reserved optical carrier and DSB modulated by uplink data. Since the initial phase θ_3 which the LSB has earned at the CS just matches the phase difference which will be produced between the LSB and the $(\omega_0 - \omega_{LO} - \omega_S)$ data sideband while the two tones travel back to the CS, the CD of the uplink can also be completely compensated (Fig. 3).

In order to verify our proposed scheme, a concept-proof ROF link can be built based on the VPI or OptiSystem platform.

The lightwave with central frequency of 193.1 THz and linewidth of 0.1 MHz is emitted from a continuous-wave LD. The MZM with an extinction ratio of 30 dB and a half-wave voltage of 4 V is driven by 20 GHz LO with a peak-to-peak voltage of 1 V. The output of the MZM consists of the LSB of 193.08 THz and the USB of 193.12 THz with a frequency spacing of 40 GHz. The USB is SSB modulated by 20 GHz 16 QAM downlink

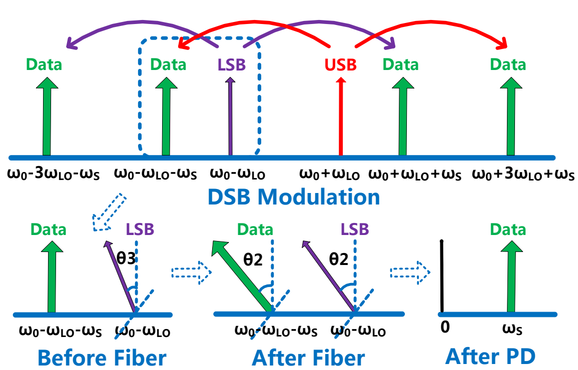

Fig. 3. Illustration of CD compensation for uplink.

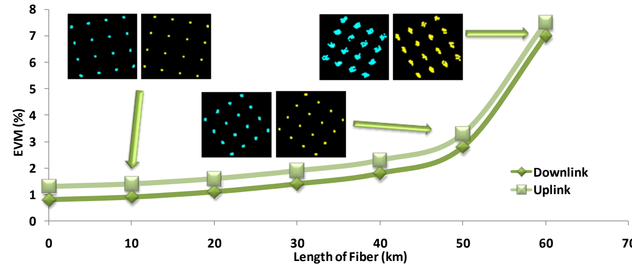

Fig. 4. Full-duplex ROF link with 5 Gb/s 16 QAM without CD compensation, blue constellation for downlink, yellow constellation for uplink.

data, which is generated by mapping a 5 Gb/s pseudo-random binary sequence to 16-ary vector signal, and modulated on 20 GHz IF carrier. The CS can be simplified and cost-effective since the carrier of the downlink data can also share the 20 GHz LO. The LSB earns an initial phase through an OPS for CD compensation. The three tones transmitted to the BS over standard SMF with a CD of 17 ps/nm/km and a power attenuation of 0.2 dB/km. At the BS, the lightwaves are power split for downlink and uplink, and a high-speed PD is used to detect the downlink optical signal. The responsivity and dark current characteristics of the PD are 1 A/W and 10 nA. For the uplink, the USB and LSB are filtered out as the reserved 40 GHz uplink optical carrier, which are DSB modulated by 5 Gb/s 16 QAM uplink data at 60 GHz. Considering the cost of the BS, we place another BPF between MZM and PD at CS instead of BS.

The impact of CD-induced CR on a ROF link is investigated (Fig. 4). Firstly, the OPS is operating with no phase shift led to the LSB. By altering the length of the SMF from zero to 60 km, various CDs are introduced into the system. Referring to the constellation of the transmitted vector signal, significant CR could be observed in both downlink and uplink. Afterward, the OPS is employed for CD compensation (Fig. 5). The CD-induced CR has received significant amelioration thanks to the OPS.

Error vector magnitude (EVM) is normally used to evaluate the performance of vector signal transmission. As is shown in Figs. 4 and 5, EVM increases gradually as the fiber CD grows, which is less than 3% within 50 km fiber transmission. Then, EVM jumps to 7% after 60 km signal transmission due to the deterioration of transmission link. Moreover, EVM of uplink is higher since the LSB travels both downlink and uplink and suffers more than only transmitted through downlink.

In conclusion, we theoretically demonstrate the impact of the CD-induced CR in ROF link with vector signal transmission and an OPS method for compensation. A 60 GHz full-duplex ROF link with vector signal transmission including no CD effect is accomplished accordingly. The evaluation of 5 Gb/s 16 QAM signal transmission shows that the CD-induced CR is entirely

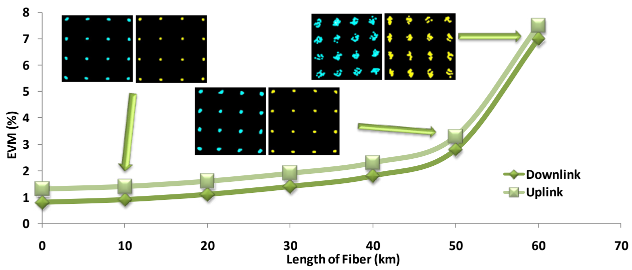

Fig. 5. Full-duplex ROF link with 5 Gb/s 16 QAM and CD compensation, blue constellation for downlink, yellow constellation for uplink.

overcome thanks to our method which can be simply implemented through an OPS, and the proposed ROF schedule still maintains good performance after 50 km transmission. Moreover, CS is significantly simplified and cost-effective since only one 20 GHz LO is needed for both the generation of an optical millimeter wave and the carrier of downlink signal. Finally, it is worth mentioning that the proposed ROF link is not only fit for V-band (57–64 GHz) but is also applicable for W-band (75–110 GHz), or any other bandwidth.

This work was supported by the National “973” Project of China (Nos. 2010CB328202, 2010CB328204, and 2012CB315604), the National Natural Science Foundation of China (Nos. 61271191 and 61001124), the National “863” Project of China (No. 2012AA011302), the Program for New Century Excellent Talents in University (No. NCET-12-0793), the Beijing Nova Program (No. 2011065), and the Fundamental Research Funds for the Central Universities.

References

1. Z. Cao, L. Zou, L. Chen, and J. Yu, J. Opt. Commun. Networking **3,** 758 (2012).
2. J. Ma, Y. Zhan, M. Zhou, H. Liang, Y. Shao, and C. Yu, J. Opt. Commun. Networking **4,** 557 (2012).
3. Z. Cao, J. Yu, M. Xia, Q. Tang, Y. Gao, W. Wang, and L. Chen, J. Lightw. Technol. **28,** 2423 (2010).
4. K. Wang, X. Zheng, H. Zhang, and Y. Guo, IEEE Photon. Technol. Lett. **19,** 1365 (2007).
5. Z. Cao, J. Yu, L. Chen, and Q. Shu, IEEE Photon. Technol. Lett. **24,** 827 (2012).
6. K. Xu, R. Wang, Y. Dai, F. Yin, J. Li, Y. Ji, and J. Lin, Photon. Res. **2,** B54 (2014).
7. Z. Guo, H. Tian, X. Wang, and Y. Ji, Photon. Res. **2,** B40 (2014).
8. S. Zhang, X. Zou, H. Wang, Y. Zhang, H. Li, and Y. Liu, Photon. Res. **2,** B26 (2014).
9. T. Hu and X. Sun, Chin. Opt. Lett. **11,** 070602 (2013).
10. Y. Jiang, S. Zhou, R. Wu, J. Li, X. Li, and Z. Lin, Chin. Opt. Lett. **11,** 081404 (2013).
11. W. Liang, N. Liu, Z. Li, and P. Lu, Chin. Opt. Lett. **11,** S20604 (2013).
12. Y. Cui, K. Xu, J. Dai, X. Sun, Y. Dai, Y. Ji, and J. Lin, IEEE Photon. Technol. Lett. **24,** 1173 (2012).
13. H. Zhang, S. Pan, M. Huang, and X. Chen, Opt. Lett. **37,** 866 (2012).
14. J. Ma, J. Yu, C. Yu, X. Xin, J. Zeng, and L. Chen, J. Lightw. Technol. **25,** 3244 (2007).
15. S. A. Havstad, A. B. Sahin, O. H. Adamczyk, Y. Xie, and A. E. Willner, IEEE Photon. Technol. Lett. **12,** 1052 (2000).
16. K. Kimura, S. Ebisawa, and J. Maeda, in *Proceedings of Microwave Photonics* 142 (2013)